Improvements in Iterative Convergence of FUN3D Solutions

Li Wang[1], Boris Diskin[2], Eric Nielsen[1], and Yi Liu[2]

[1] NASA Langley Research Center
[2] National Institute of Aerospace
Hampton, VA, USA

AIAA SciTech Forum and Exposition 2021
January 14, 2021

Copyright 2021 National Institute of Aerospace and United States Government as represented by the Administrator of the National Aeronautics and Space Administration. Published by the American Institute of Aeronautics and Astronautics, Inc., with permission. All other rights reserved.

Overview



Computational Fluid Dynamics (CFD) Plays a Growing Role in Aerospace Analysis and Design

- Effectiveness is largely driven by its reliability and efficiency
- Challenges may arise with more complicated physics involved
- Key aerodynamic quantities can show insufficient convergence
- Strong solver technology demanded for robustness, accuracy, and efficiency of CFD solutions

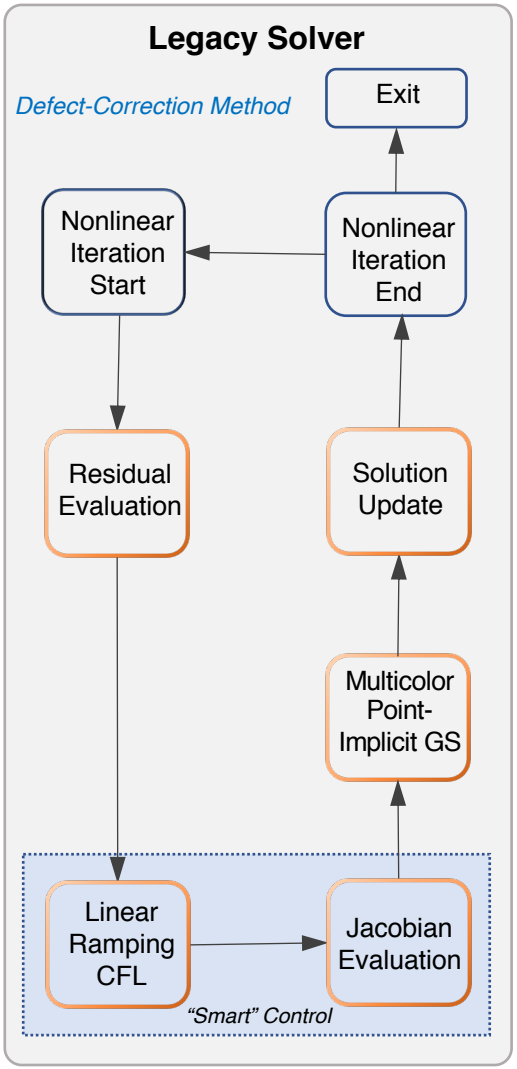
Objectives

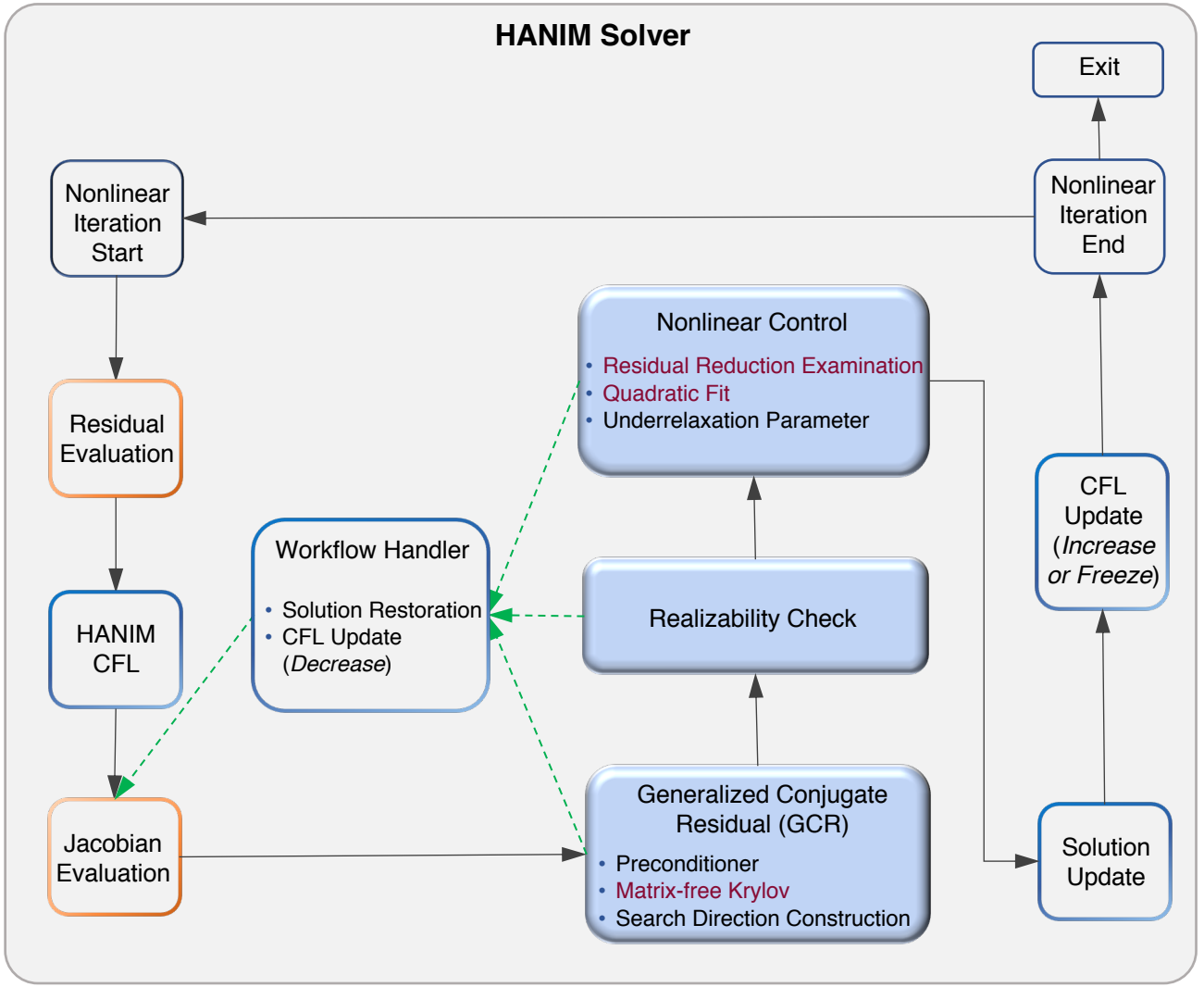
- Investigate a hierarchical adaptive nonlinear iteration method (HANIM) to improve reliability and efficiency of CFD solutions
- Implement HANIM solver in NASA's FUN3D code based on unstructured-grid, node-centered, finite-volume discretizations
- Compare HANIM computational efficiency with FUN3D legacy solver

HANIM Applications

- Steady and unsteady Reynolds Averaged Navier-Stokes (RANS) equations with one-equation turbulence models
- Static, dynamic, overset grid simulations
- Low-speed, subsonic, transonic, and supersonic flows
- Present assessment focused on steady flow simulations

Methodology

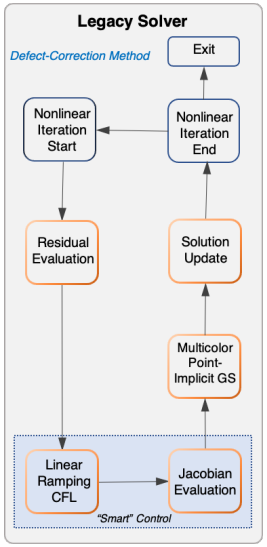


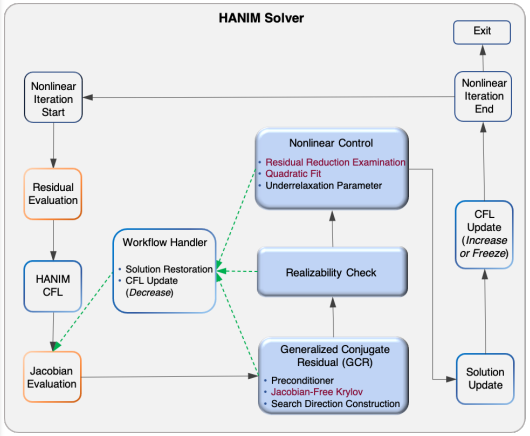


- *Pseudotime term added to diagonal of Jacobian, controlled by CFL*
- *Detailed mathematical formulations provided in paper*
- *Red texts indicate multiple residual evaluations may be required*
- *Green dashed arrows show workflow when HANIM module fails*

Key Elements

Elements	Legacy	HANIM
Residual	Second-order inviscid, Roe flux Second-order viscous, Green-Gauss gradients with face-tangent augmentation SA-neg	Second-order inviscid, Roe flux Second-order viscous, Green-Gauss gradients with face-tangent augmentation SA-neg
Jacobian Construction	First-order inviscid, VanLeer flux Second-order viscous Linear ramping CFL	First-order inviscid, Roe flux Second-order viscous Adaptive CFL
Jacobian Update	"Smart" control	Every nonlinear iteration
Preconditioner	Multicolor point-implicit GS	Multicolor point-implicit GS
Gauss-Seidel Sweeps	Fixed, 15 for meanflow equations, 10 for turbulence-model equation (default)	Varying depending on maximum preconditioner iterations & tolerance
GCR & Nonlinear Control	—	Multiple residual evaluations, Pseudotime Jacobian update when CFL reduced
Realizability Check	Cutoff using minimum allowable pressure/density	Nodal pressure/density realizability
Solution Update	Full or underrelaxation based on magnitude of solution update	Full or underrelaxation (quadratic fit)





Key Elements

Elements	Legacy	HANIM	Preconditioner Alone (PA)
Residual	Second-order inviscid, Roe flux Second-order viscous, Green-Gauss gradients with face-tangent augmentation SA-neg	Second-order inviscid, Roe flux Second-order viscous, Green-Gauss gradients with face-tangent augmentation SA-neg	Second-order inviscid, Roe flux Second-order viscous, Green-Gauss gradients with face-tangent augmentation SA-neg
Jacobian Construction	First-order inviscid, VanLeer flux Second-order viscous Linear ramping CFL	First-order inviscid, Roe flux Second-order viscous Adaptive CFL	First-order inviscid, Roe flux Second-order viscous Linear ramping CFL
Jacobian Update	"Smart" control	Every nonlinear iteration	Every nonlinear iteration
Preconditioner	Multicolor point-implicit GS	Multicolor point-implicit GS	Multicolor point-implicit GS
Gauss-Seidel Sweeps	Fixed, 15 for meanflow equations, 10 for turbulence-model equation (default)	Varying depending on maximum preconditioner iterations & tolerance	Fixed, 15 for meanflow equations, 10 for turbulence-model equation (default)
GCR & Nonlinear Control	—	Multiple residual evaluations, Pseudotime Jacobian update when CFL reduced	—
Realizability Check	Cutoff using minimum allowable pressure/density	Nodal pressure/density realizability	Cutoff using minimum allowable pressure/density
Solution Update	Full or underrelaxation based on magnitude of solution update	Full or underrelaxation (quadratic fit)	Full or underrelaxation based on magnitude of solution update

Numerical Examples

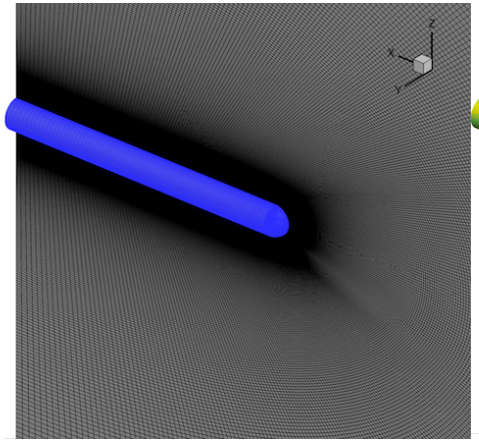
- Subsonic Flow over a Hemisphere Cylinder
  - Linear one-equation turbulence model (SA-neg)
- Supersonic Flow in a Long, Square Cross-Section Duct (*shown in paper*)
  - Nonlinear one-equation turbulence model with quadratic constitutive relation (SA-neg-QCR2000)
- Subsonic Flow over NASA's Wing-Fuselage Junction Configuration
  - SA-neg-QCR2000 turbulence model

Subsonic Flow over Hemisphere Cylinder

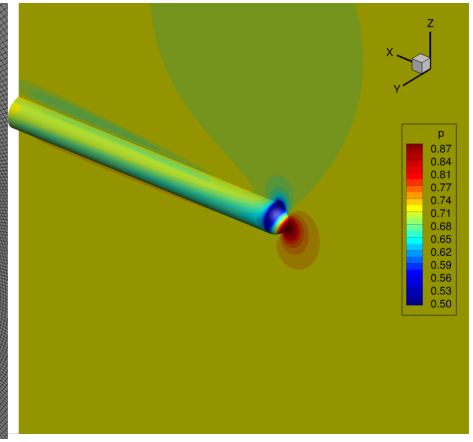
Flow Conditions: M_∞ = 0.6, AoA = 19°, Re_D = 350,000

Linear SA-neg turbulence model

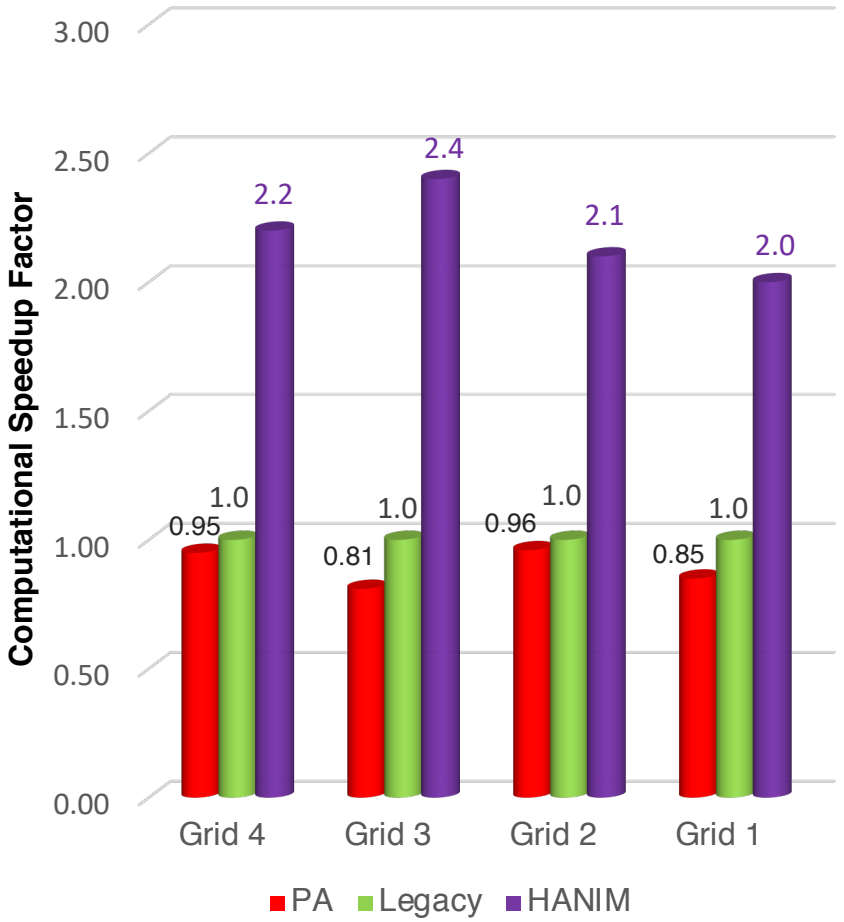
Grid	Nodes	Cells	Prisms / Hexahedra
4	147,637	153,600	30,720 / 122,880
3	1,143,081	1,228,800	245,760 / 983,040
2	8,995,153	9,830,400	1,966,080 / 7,864,320
1	71,368,353	78,643,200	15,728,640 / 62,914,560



Grid 2



Pressure



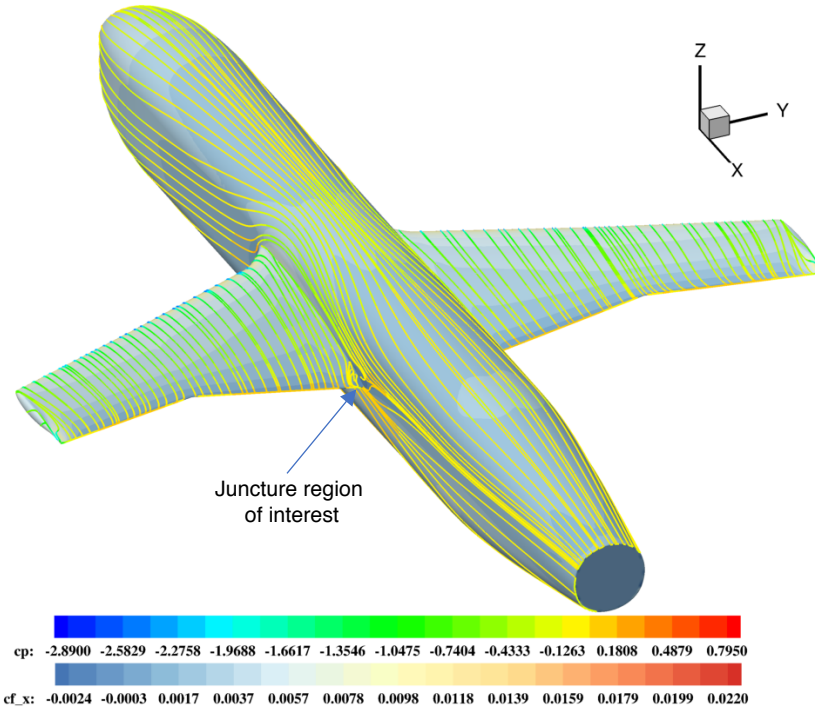
- Nonlinear residual convergence target (for all solvers): 10^{-13}
- HANIM achieved **2.0-2.4x** speedup over legacy solver and 2.1-2.6x over PA solver

NASA Juncture Flow Model Simulations

Flow Conditions: $M_\infty = 0.189$, AoA = 5°, $Re_L = 4307.45$

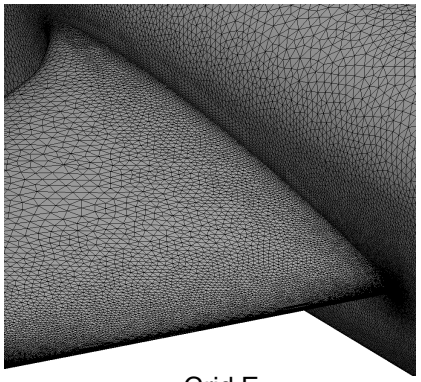
SA-neg-QCR2000 turbulence model

Configuration and Computational Grids

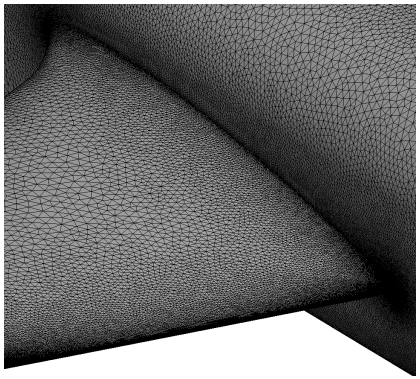


- Nonlinear residual convergence target (for all solvers): 1.510^{-10}

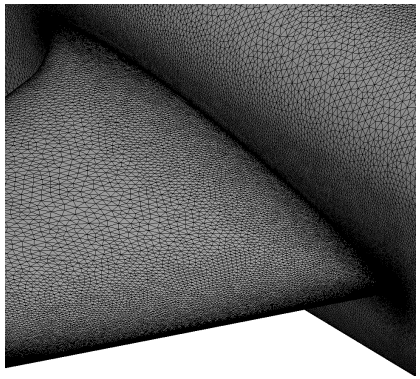
Grid	Nodes	Cells	Tetrahedral / Pyramids / Prisms
E	4,784,640	10,785,042	5,952,907 / 47,495 / 7,479,778
I	13,036,210	37,126,819	16,645,072 / 112,989 / 20,368,758
P	37,131,844	113,428,664	58,432,891 / 227,396 / 54,768,377
V	106,090,663	420,167,293	307,693,938 / 374,233 / 112,099,122



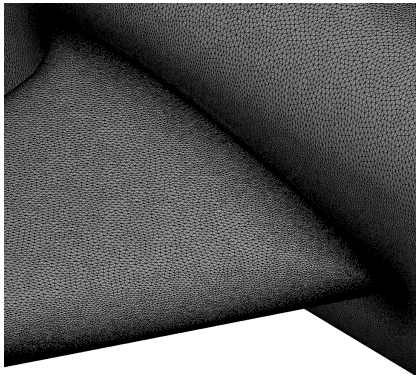
Grid E



Grid I



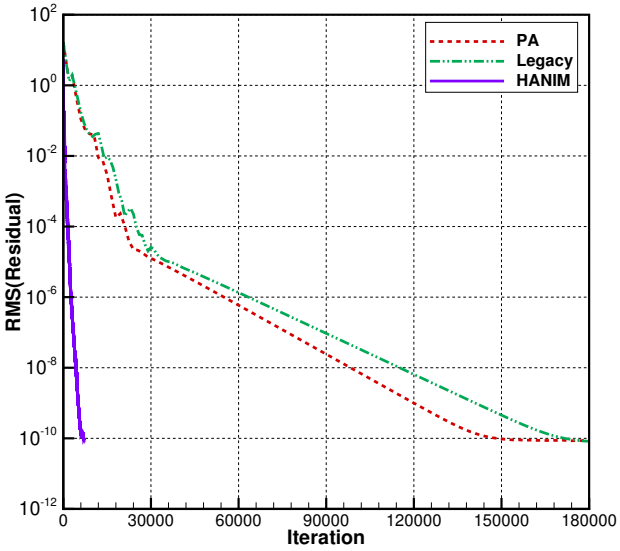
Grid P

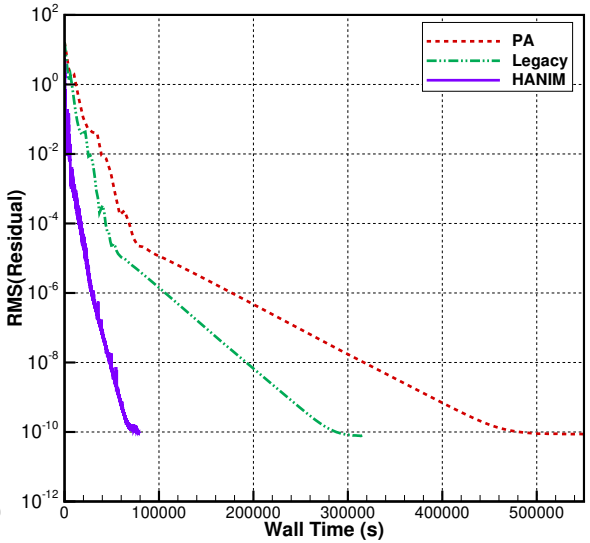


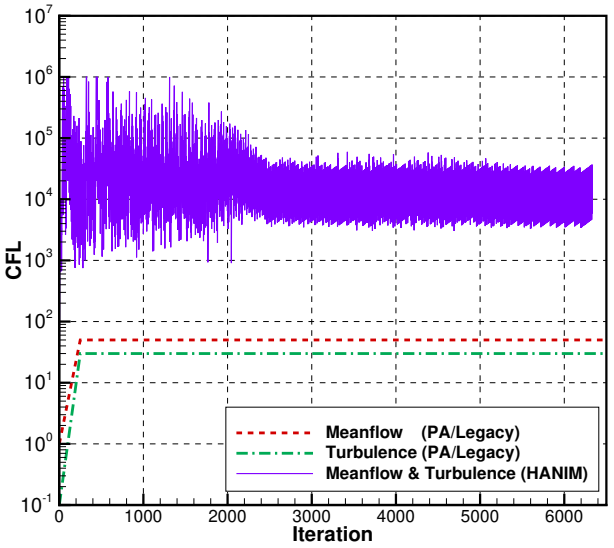
Grid V

Nonlinear Iterative Convergence

Grid I (13M Nodes)



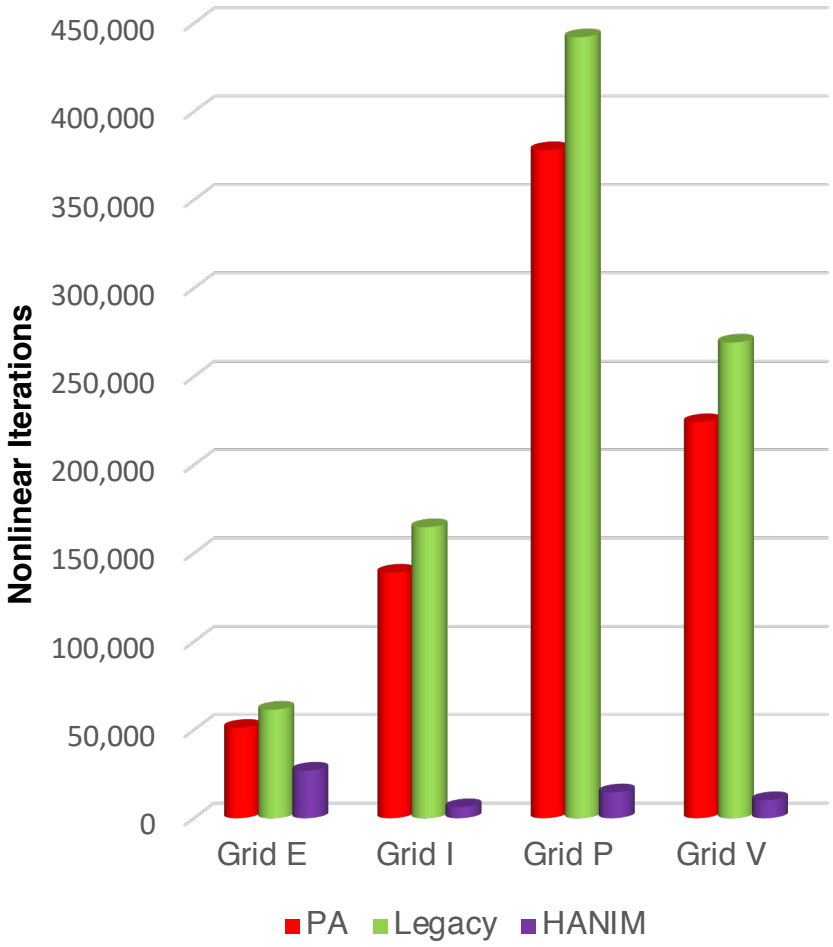


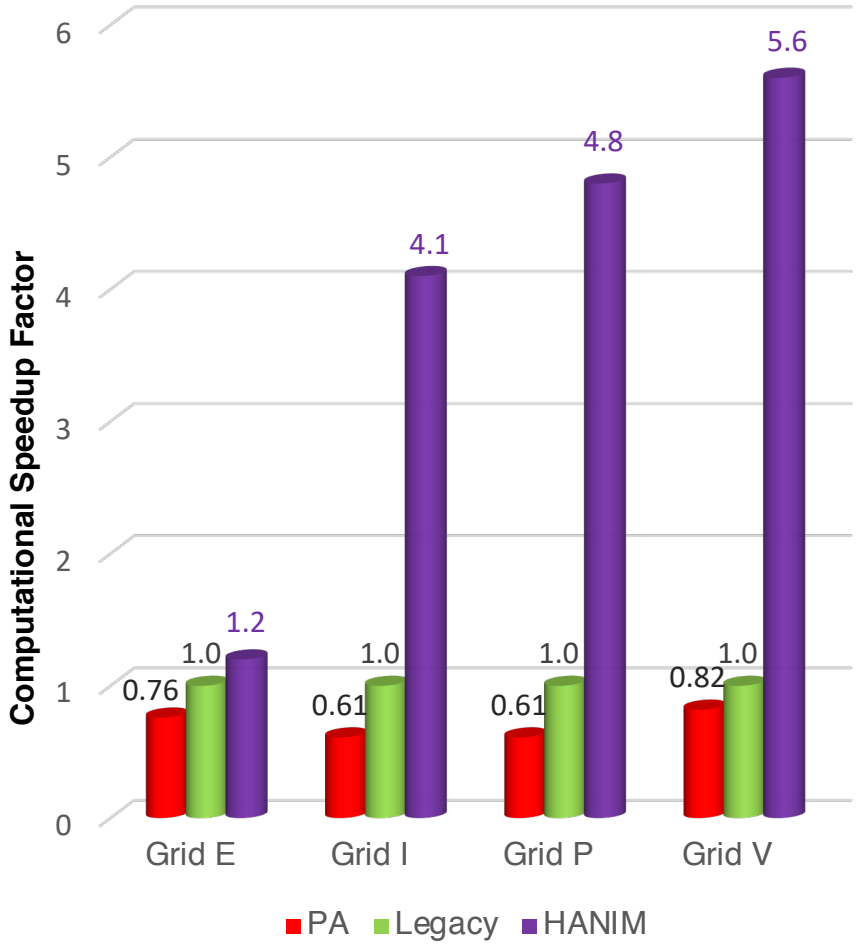


Assessment of HANIM Solver

- 1-2 orders of magnitude (OOM) fewer nonlinear iterations than Legacy/PA to achieve convergence
- 5 OOM more residual reductions than Legacy/PA when reaching residual convergence target
- Several OOM higher CFL numbers

Performance Assessment



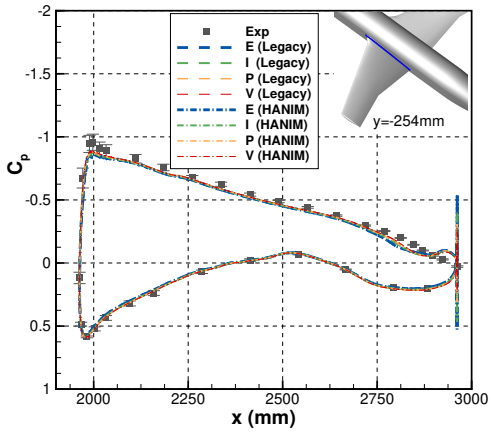


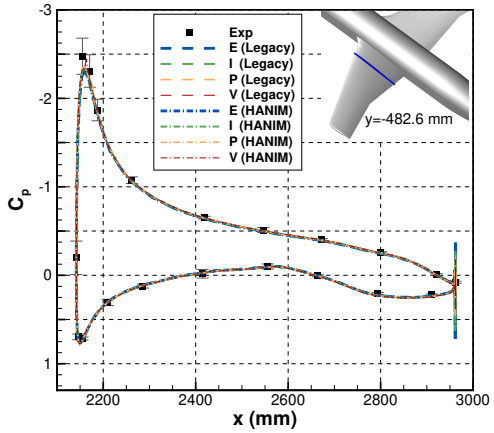
- Target residual convergence level: $1.5 10^{-10}$

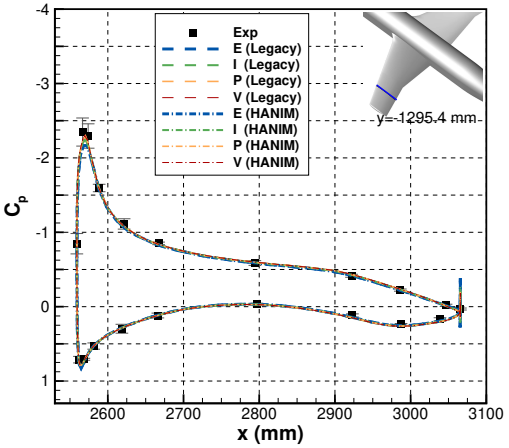
- HANIM achieved **1.2-5.6x** speedup over legacy solver and **1.6-7.8x** speedup over PA solver

Aerodynamic Predictions

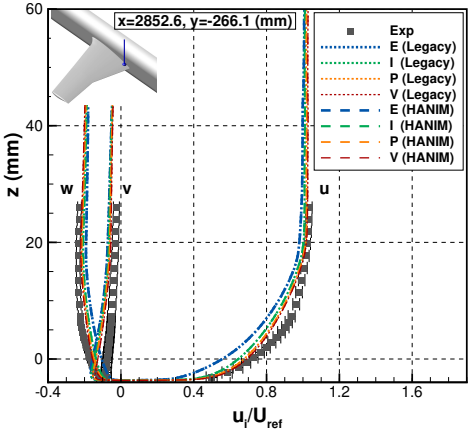
Surface Pressure

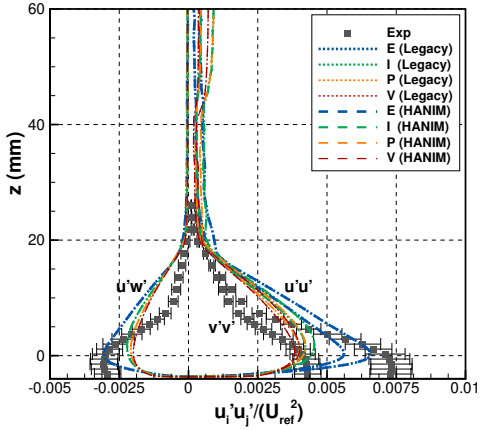


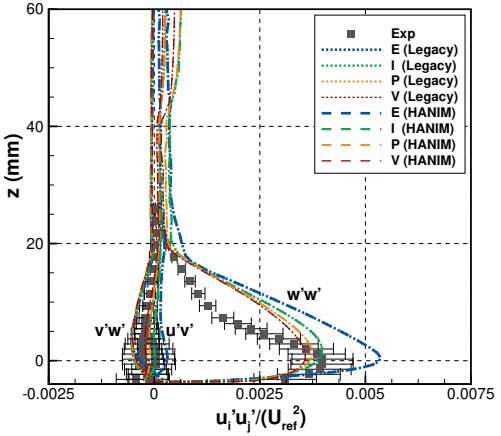




Velocity and Reynolds Stresses







- HANIM and legacy solvers produced identical solutions
- Predicted solutions compare well with experimental measurements
- *Additional data provided in the paper*

Conclusion

- HANIM implemented in NASA computational fluid dynamics solver, FUN3D
  - Hierarchy of solution modules including preconditioner, GCR, realizability check, nonlinear control, and CFL adaptation modules
- HANIM demonstrated for three benchmark problems
  - Subsonic separated flow around a hemisphere-cylinder (HC) configuration
  - Supersonic flow through a long square duct (SD, *shown in paper*)
  - Subsonic flow over the NASA juncture-flow model (JFM)
- HANIM compared with legacy and preconditioner-alone (PA) solvers
  - Fewer nonlinear iterations
  - Orders of magnitude higher CFL
  - Moderate speedup of ***1.6-2.4x*** for HC and SD
  - Superior performance for JFM with speedup of ***4.1-5.6x***
- HANIM future directions
  - Future improvements in efficiency and robustness
  - Extension to GPU architectures and reacting-flow simulations

Acknowledgments

The work is supported by:

NASA Revolutionary Vertical Lift Technology (RVLT) Project

NASA Revolutionary Computational Aerosciences (RCA) Project

NASA Langley High Performance Computing Incubator (HPCI) Program

Computations were performed on the NASA LaRC K-Cluster and NASA Advanced Supercomputing Pleiades system.

The authors would also like to thank Dr. Steve Karman (Pointwise Inc.), and Drs. Mike Park, Nashat Ahmad, Kyle Anderson, and Mohagna Pandya (NASA LaRC).